Chemistry & Biology Interface, 2024, 14, 2, 40-53

RESEARCH PAPER ISSN: 2249 –4820

CHEMISTRY & BIOLOGY INTERFACE

An official Journal of ISCB, Journal homepage; www.cbijournal.com

Green Synthesis of Tellurium-Loaded CuO/Ag/Gd_2O_3 Polymetallic Nanoparticles Using Justicia adhatoda Extract: Enhanced Photocatalytic, Antibacterial, and Antimalarial Properties

Rathika Radhakrishnan, Srinivasan Subramanian*.

Department of Chemistry,Annamalai University,Chidambaram,Tamil Nadu.
Rathika Radhakrishnan , Department of Chemistry, Annamalai University.
Srinivasan Subramanium, Associate Professor,Department of Chemistry, Annamalai University.
Email:rathikaradha1997@gmail.com , drssvasan74@rediffmail.com
Received; 31 March 2024, Accepted;22 April 2024

Abstract: The objective of this study is to synthesize biologically derived CuO, Ag, and Gd_2O_3 polymetallic nanoparticles (NPs) using Justicia adhatoda bark extract. These nanoparticles were meticulously prepared and characterized through a comprehensive array of spectral analyses, including UV-Visible, FTIR, SEM, EDX, XRD, and thermal studies. UV-Vis spectroscopy revealed distinct absorption peaks in the 200–300 nm range, indicative of the presence of metal oxide nanoparticles. FTIR studies elucidated the interactions between bioorganic compounds and the synthesized NPs. SEM and XRD analyses provided insights into the crystallinity, crystal structure, and morphologies of the nanoparticles. Thermal properties, such as decomposition rates and transition energies, were examined via TGA/DTA. Notably, the PNs exhibited enhanced photocatalytic activity against methylene blue (MB) compared to individual NPs. Additionally, they demonstrated potent antibacterial effects against human pathogens and remarkable antimalarial activity against Aedes aegypti across various concentrations. The novelty of this work lies in the utilization of Justicia adhatoda bark extract for the green synthesis of multifunctional PNs with enhanced properties for diverse applications.

1.1.INTRODUCTION:

The growing need for environmentally friendly and sustainable synthesis methods has spurred the investigation into biologically mediated approaches for crafting advanced nanomaterials. Malaria, a life-threatening disease transmitted to humans by certain species of mosquitoes, predominantly afflicts populations in tropical regions. Despite its severity, malaria remains both preventable and treatable, as it is a non-communicable disease—meaning the infection does not spread directly from person to person [1,2].

The burgeoning field of nanotechnology has witnessed a surge in interest towards sustainable and environmentally friendly synthesis methodologies, driven by the imperative to mitigate environmental impacts and enhance the biocompatibility of nanomaterials. Among these approaches, green synthesis stands out for its utilization of natural

resources and bio-based materials to fabricate nanomaterials with tailored properties and diverse applications[3,4]. One notable application area is in the realm of healthcare and environmental remediation, where nanomaterials have demonstrated immense potential in combating diseases and pollution[5].

Malaria, a life-threatening disease transmitted by Anopheles mosquitoes infected with Plasmodium parasites, remains a significant public health concern, particularly in tropical and subtropical regions[6,7]. Despite concerted efforts to control the spread of malaria, the disease continues to exact a heavy toll on human health and well-being. The development of effective antimalarial strategies is therefore imperative to combat this global health challenge[8,9].

In the pursuit of advancing nanomaterials tailored for applications in photocatalysis, antibacterial interventions, and antimalarial treatments, the exploration of polymetallic nanoparticles (PNs) stands out for its potential to deliver enhanced efficacy. PNs, characterized by their amalgamation of diverse metallic elements, offer unique physicochemical properties and synergistic effects that render them versatile candidates for various biomedical and environmental applications[10,11].

Notably, metal oxides such as copper oxide (CuO), silver (Ag), gadolinium oxide (Gd_2O_3) and tellurium nanoparticles have garnered significant attention for their catalytic prowess, antimicrobial activity, and utility in biomedical settings[12,13].

The employment of natural extracts as both reducing and stabilizing agents in the synthesis of metal and metal oxide nanoparticles presents numerous advantages, including cost-effectiveness, environmental sustainability, and scalability[14].

Among these natural sources, Justicia adhatoda, known by various names including Adhatodavasica or Vasaka, holds a prominent place due to its well-established therapeutic properties in traditional medicine systems[15,16].

The bioactive constituents found within Justicia adhatoda extract possess inherent abilities to reduce and cap nanoparticles, making it a promising candidate for green synthesis endeavors[17].

In this study, we present a novel approach to the green synthesis of tellurium-loaded $CuO/Ag/Gd_2O_3$ PNs utilizing Justicia adhatoda extract as a reducing and stabilizing agent. Through meticulous characterization employing an array of spectroscopic and microscopic techniques, we elucidate the structural, morphological, and thermal properties of the synthesized nanoparticles.

Furthermore, we evaluate the photocatalytic, antibacterial, and antimalarial activities of the PNs to gauge their potential applications in both biomedical and environmental contexts. This research not only contributes to the burgeoning field of green nanotechnology but also holds promise for the development of sustainable solutions to address pressing healthcare and environmental challenges.

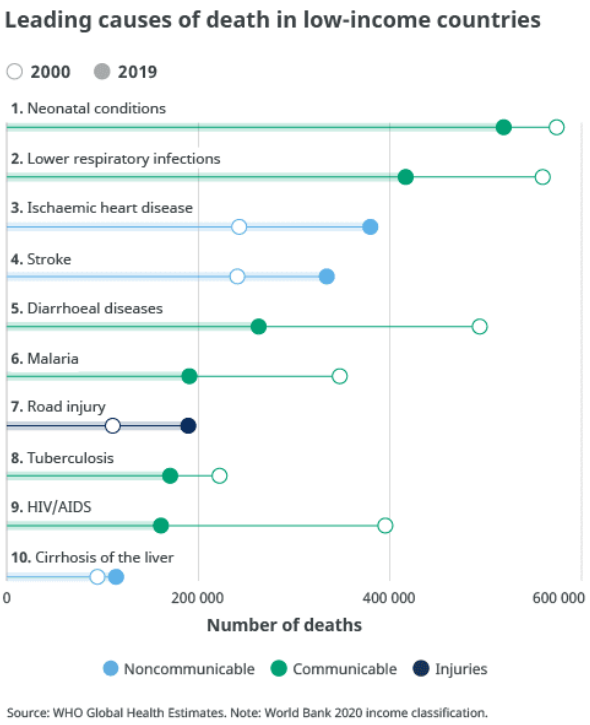

2. Experimental Section

2.1. Materials

Copper sulfate ($CuSO_4.6H_2O$), silver nitrate ($AgNO_3$), gadolinium chloride hexahydrate ($GdCl_3.6H_2O$), and potassium tellurite hydrate ($K_2TeO_3.H_2O$) were brought from the Siscochem laboratory for analytical standards.

2.2.Instrumentation

The biologically prepared Te-loaded polymetallic NPs were primarily confirmed using UV-visible spectral studies. It was examined using UV-visible spectroscopy (SHIMADZU-UV 1800). Quartz (10 mm) was used. The application of the instrument is to determine the qualitative (functional) and quantitative (concentration) information of a substance by means of the distinct surface plasmon resonance patterns that were obtained.

The FTIR spectra used to determine the various biochemical compounds that are responsible for the bioreduction of metal ions act as stabilizing or capping agents. Moreover, the interaction of metal nanoparticles is also known [18]. The broad peaks obtained correspond to functional groups such as phenols,alkaloids, ketones, etc[19].

The scanning electron spectroscopy with EDX mode (JEOL-JSM-IT200) with an accelerating voltage of 0.5 kV to 30 kV The maximum frequency size is 32mm dia x 10 mm H, with a resolution of 3.0 LV and 4.5 LV and a magnification range of X18 to 3,00,0000. It gives information about the shape, structure, and other topographical and compositional features of the samples that were employed for analysis.

Te-loaded PNs can be studied using an X-ray diffraction spectrometer. It provides the crystallographic properties of solid, liquid, and gaseous materials. The crystal structure, lattices,shape, phase orientation, and crystal orientations. We can calculate the size of the NPs from these studies.

2.3. Preparation of Te-loaded CuO/ Ag/Gd_2O_3 polymetallic nanoparticles (PNs):

The synthesis process comprises two steps. Firstly, approximately 12g of fresh bark from Justicia aduthoda was gathered, thoroughly washed with tap water to eliminate debris and impurities, and subsequently air-dried at room temperature. Subsequently, 250 ml of

double-distilled or deionized water was added to the dried bark and boiled for one hour to produce the bark extract. Following boiling, the extract was filtered, collected in an iodine flask, and left undisturbed overnight. At the conclusion of this step, the initially colorless solution transitioned to a straw-yellow hue, which was then filtered using Whatmann filter paper.**2.1.**

In the subsequent step, approximately 30 ml each of 0.01 M copper sulfate ($CuSO_4.6H_2O$), silver nitrate ($AgNO_3$), gadolinium chloride hexahydrate ($GdCl_3.6H_2O$), and potassium tellurite hydrate ($K_2TeO_3.H_2O$) were heated to 70°C and maintained at this temperature for over 2 hours. Concurrently, 100 ml of the bark extract was combined with the metal precursor solutions at room temperature, utilizing a magnetic stirrer for thorough mixing. Instantaneously, the straw-yellow solution transformed into a vibrant magenta color, indicative of nanoparticle formation. The resultant precipitate was then collected, filtered, washed successively with double-distilled or deionized water, and ethanol. Subsequently, it was subjected to drying in a hot air oven at 150°C for 2 hours to ensure complete evaporation of solvents and stabilization of the nanoparticles, preparing them for subsequent characterization analyses.

3. Results and Discussion

3.1. Characterization

This study quantitatively confirms the formation of polymetallic nanoparticles (PNs) through the observation of surface plasmon resonance within the 200–300 nm range. The emergence of multiple absorption peaks corresponding to Cu, Ag, Gd, and Te nanoparticles further validates their formation. Additionally, the visual transition of the solution from straw yellow to bright magenta, accompanied by spectral data presented in Fig. 1, provides clear evidence of the formation of tellurium-loaded CuO, Ag, and Gd_2O_3 PNs.

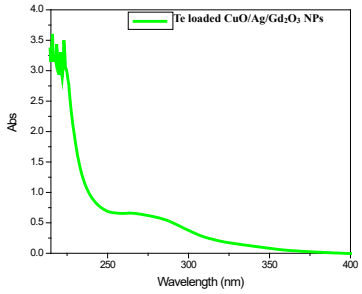

Fig3.1:UV-Vis spectra of Te Loaded CuO/Ag/Gd_2O_3PNs.

Figure 2 displays the FTIR spectra of the polymetallic nanoparticles (PNs) within a spectral range of 600–4000 cm^{-1}. The spectra exhibit distinct bands at 3360, 2900, 1720, 1660, and 1160 cm^{-1}, corresponding to the stretching vibrations of O-H, C-H, C=O, C=C, and C-O, respectively. These bands indicate the presence of various bioorganic molecules, including phenols, amino acids, and carboxylic acid compounds, as previously reported by Shaimaa Hussain et al. The band observed at 3390 cm^{-1} and 1640 cm^{-1} signifies C=O stretching vibrations in carboxyl or N=O bending in the amide group of flavonoids, among other compounds, while the band around 1590 cm^{-1} corresponds to the N-H band of primary amines present in the mixed bark extract of J. adhatoda[20]. The overlapping bands in the spectra arise from the diverse bioorganic compounds present in both the extract

and the PNs. Additionally, bands below 600 cm^{-1} are attributed to metal-metal interactions within the PNs, whereas those around 2900 cm^{-1} correspond to stretching frequencies of alcohol and phenol functionalities.FTIR analysis of the polymetallic nanoparticles (PNs) revealed characteristic absorption bands corresponding to functional groups present in both the Justicia adhatoda extract and the synthesized nanoparticles. These spectra confirm the successful incorporation of bioorganic compounds onto the nanoparticle surface and provide insights into the chemical composition and structural properties of the PNs.

The observed bands suggest the presence of diverse biomolecules, including phenols, amino acids, and carboxylic acids, contributing to the stability and functionality of the synthesized nanoparticles. Overall, FTIR analysis serves as a valuable tool for elucidating the molecular interactions and confirming the formation of functionalized PNs.

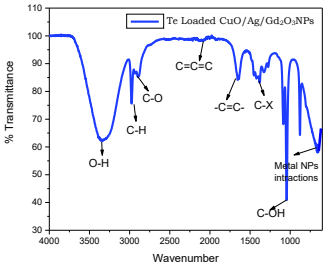

Figure 3.2: FT-IR spectra of Te-loaded CuO/Ag/Gd_2O_3NPs.

The SEM analysis, conducted at varying magnification levels (1500X, 5000X, 10,000X, etc.), as depicted in Fig. 3, reveals the spherical morphology of the Te-loaded polymetallic nanoparticles (PNs), composed of CuO, Ag, and Gd_2O_3 NPs. Elemental compositions were further elucidated through EDX spectra, showcasing peaks of varying intensities corresponding to the metals present in the PNs. Specifically, the biologically synthesized PNs exhibit a composition comprising 48% oxygen, 8.85% copper, 11% silver, 20% tellurium, and 11.7% gadolinium. Notably, oxygen constitutes the majority (48%) of the PNs' mass, indicative of their oxidized state, as illustrated in Fig. 4. This observation underscores the susceptibility of Cu and Gd NPs to oxidation, likely attributed to the elevated temperatures employed during the PNs synthesis process.

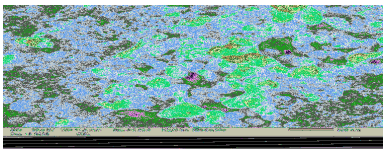

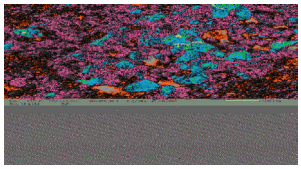

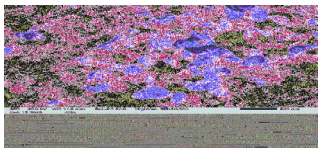

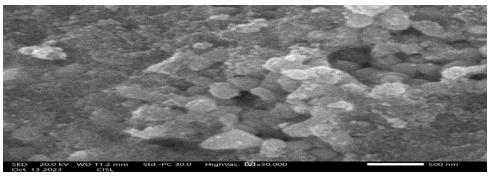

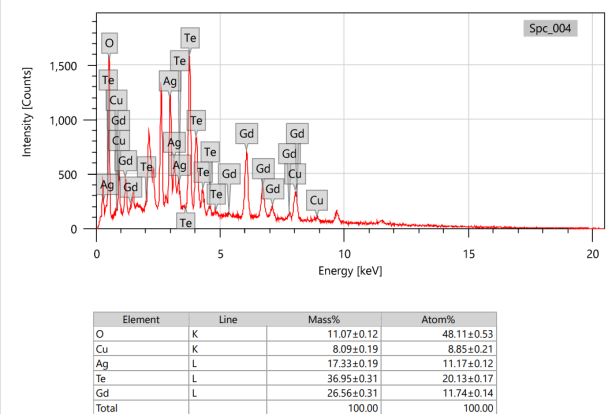

Element	Line	Mass%	Atom%
O	K	11.07±0.12	48.11±0.53
Cu	K	8.09±0.19	8.85±0.21
Ag	L	17.33±0.19	11.17±0.12
Te	L	36.95±0.31	20.13±0.17
Gd	L	26.56±0.31	11.74±0.14
Total		100.00	100.00

Fig. 3.3 and 3.4: SEM imagesEDX spectra and atom compositions of Te-loaded CuO/Ag/Gd_2O_3/Te NPs respectively.

The XRD patterns revealed broadened line patterns consistent with a space group approximately Fm-3m and a lattice parameter of a = 4.02 (4 Ag atoms in a unit cell), matching JCPD file no. 04-0783. These broad patterns arise from both crystalline size and lattice strain [21]. Notably, small, distinct peaks at 32.50, 35.30, 38.70, 580, 61.50, and 66.20 correspond to (110), (002), (202), (113), and (311) planes of the face-centered cubic structure in silver nanoparticles (Ag NPs).

CuO NPs were found to exhibit a monoclinic phase with a face-centered structure, consistent with JCPDS No. 45-6937. The average particle size of CuO NPs was observed to be in the range of 10–25 nm [22]. On the other hand, Gd2O3 NPs displayed distinctive peaks at 2θ = 20.080, 28.560, 33.100, 47.500, and 56.350, corresponding to (211), (222), (400), (440), and (622) planes, respectively, indicating a cubic structure with an average size of approximately 30–50 nm [JCPDS NO: 01-074-8036] [23].

Tellurium nanoparticles (Te NPs) exhibited a hexagonal phase, with observed peak positions corresponding to (100), (101), (102), (201), (202), (212), and (211) planes, consistent with JCPDS No. 36-1452 [24].

Additionally, lattice constants calculated from the diffraction patterns closely matched literature values, with α = 4.4 and β = 5.9 [21].

The Debye Scherrer equation ($d=k\lambda/\beta\cos\theta$) facilitated the calculation of the average sizes of all nanoparticles, where d represents particle size in nm, k is the Scherrer constant, β is the full width half maximum, θ is half of Bragg's angle, and λ is the wavelength of x-ray [25].

XRD analysis elucidated the crystalline structures and average particle sizes of the synthesized nanoparticles, confirming their distinct phases and morphologies.

The observed patterns and peak positions closely matched standard references, validating the successful synthesis of polymetallic nanoparticles with tailored properties. These findings provide valuable insights into the structural characteristics and potential applications of the nanoparticles in various fields, including catalysis, antimicrobial activity, and biomedical interventions.

Overall, XRD analysis serves as a crucial tool for characterizing the structural properties of nanoparticles and guiding further research and development efforts.

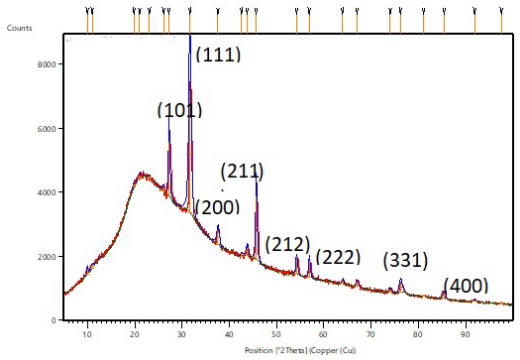

Fig. 3.5.Xrd spectra of Te-loaded CuO, Ag, and Gd2O3 NPs.

Thermal analysis was conducted to explore various thermal properties of the synthesized nanoparticles, including decomposition behavior, melting point, glass transitions, oxidation rate, degree of crystallinity, purity, energy of transition, and sample identification.

The analysis was performed using a simultaneous thermal analyzer (Model: NETZSCH-STA449F3 JUPITOR) with a wide temperature range from room temperature (RT) to 1400°C, with a heating rate of 10-20°C/min, under both liquid (10 ml) and blank atmospheres.

Approximately 50–100 mg of Te-loaded polymetallic nanoparticles (PNs) were carefully placed in an Al_2O_3 crucible for the analysis. The thermal profile ranged from a minimum temperature of 200°C to a maximum temperature of 700°C.

Notably, the decomposition behavior of the biologically synthesized Te-loaded Cu, Ag, and Gd/Te nanoparticles was observed around 300°C, exhibiting an exothermic nature.

Furthermore, the thermal study enabled the determination of critical thermal parameters essential for understanding the stability and behavior of the synthesized nanoparticles under various thermal conditions.

These insights are crucial for assessing the suitability of the nanoparticles for specific applications and optimizing their synthesis processes.

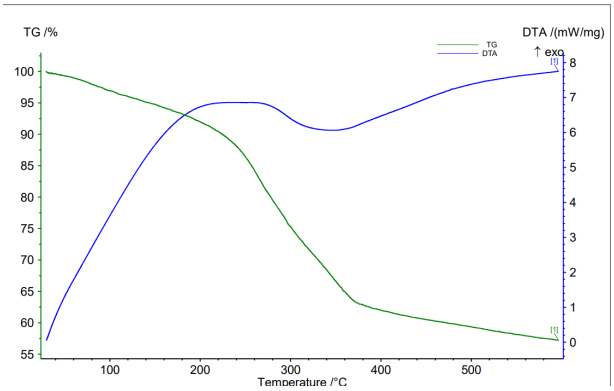

Fig.3.6. TG/DTA studies of Te-loaded CuO/Ag/Gd/Te NPs.

3.2. Photocatalytic activity of CuO/Ag/Gd/Te NPs:

The photocatalytic efficiency was evaluated using methylene blue (MB) dye as a model pollutant under a UV photoreactor. Methylene blue exhibits a characteristic absorption peak within the range of 200–400 nm. The decolorization process was initiated by subjecting the dye solution with a concentration of x 10^{-3} M to UV-light irradiation at various time intervals.

The degradation kinetics found to be dependent on both the catalyst type and irradiation duration. The dye molecules adsorbed onto the surface of the photocatalyst induce the generation of hydroxyl radicals (OH•), facilitating the degradation process. However, prolonged

exposure and increased concentration of the dye may lead to saturation of active sites on the photocatalyst surface and scavenging of free hydroxyl radicals by the polymetallic nanoparticles (PNs).

Visual observation revealed a gradual reduction in the dark blue color intensity of the MB dye over time, indicating the degradation process.

The surface transmission of electron-hole pairs initiates the formation of reactive oxygen species (ROS), which play a pivotal role in the degradation mechanism. These ROS radicals contribute to the efficient degradation of the MB dye at different time intervals, as illustrated in Fig.3.7. This photocatalytic degradation process demonstrates the potential of the synthesized PNs for environmental remediation applications.

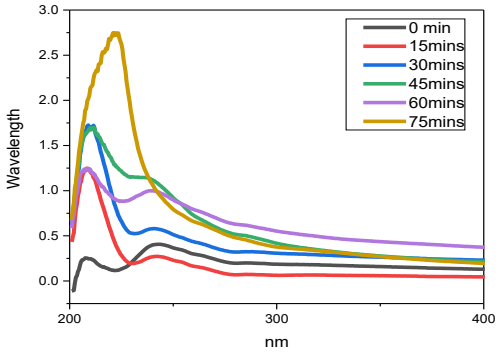

Fig. 3.7. Photocatalytic activity of Te-loaded CuO, Ag, and Gd2O3 PNs against methylene blue dye.

The catalytic activity mechanism of Te-loaded CuO/Ag/Gd2O3/Te nanoparticles involves the generation of electron-hole pairs through the induced transition from the valence band to the conduction band (CB), resulting in the creation of a hole.

Illumination of the methylene blue (MB) dye solution initiates the formation of electron-hole pairs, with the resulting hole reacting with OH ions to generate reactive OH radicals in the dye solution.

Simultaneously, the generated electrons participate in the oxygen reduction process, producing O2 radicals. Notably, the degradation of MB dye through this process is environmentally non-toxic.

The detailed mechanism, illustrated in Fig. 8, highlights the crucial role played by hydroxyl radicals (OH•), superoxide radical anions (O2•−), holes (h+), and electrons (e-) in the photocatalytic degradation of MB dye . This comprehensive understanding of the mechanism underlines the potential applications of Te-loaded CuO/Ag/Gd2O3/Te nanoparticles in the efficient and environmentally benign degradation of organic pollutants.

$CuO/Ag/Gd_2O_3/Te + h\nu$

$CuO/Ag/Gd_2O_3/Te\ (h^+)$

$H_2O + h^+$

$^0OH + H^+$

$O_2 + e^- O2^{0-}$

$^0OH + MB\ dye \rightarrow (CO_2 + H_2O)$ Degradation products.

$O_2^{\cdot -} + MB\ dye \rightarrow (CO_2 + H_2O)$ Degradation products.

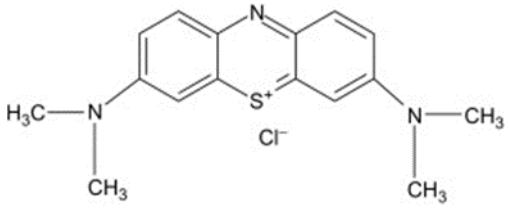

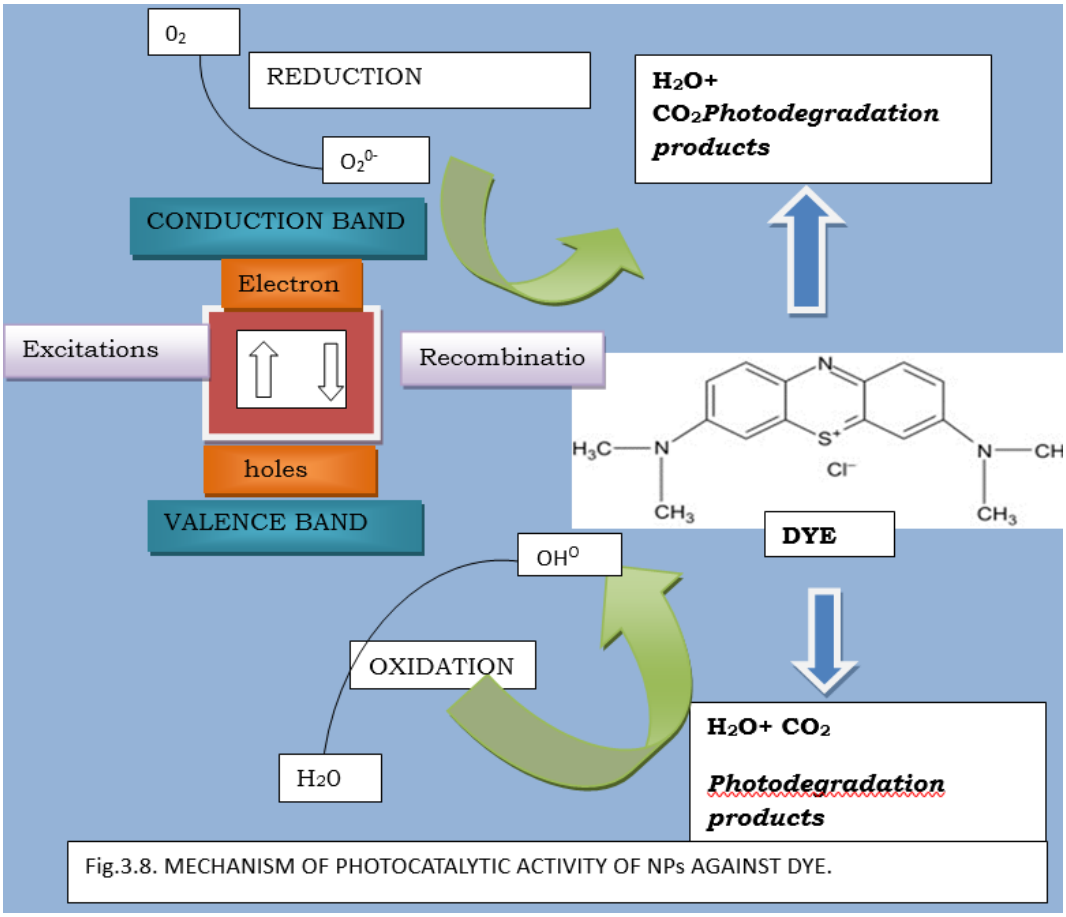

Fig.3.8. MECHANISM OF PHOTOCATALYTIC ACTIVITY OF NPs AGAINST DYE.

In the fig.3.8 depicts the mechanism of photocatalytic activity of NPs catalyst against methylene blue dye.

In the context of methylene blue (MB) dye degradation, the stability, recyclability, and efficient utilization of the catalyst are paramount. The catalyst can be easily reclaimed for subsequent use through a simple process involving centrifugation, washing, and drying at 100°C for one hour. Remarkably, the photocatalyst maintains its efficacy across multiple irradiation cycles under UV light. The exceptional reusability of these heterometallic nanoparticles has been extensively documented in the literature, exemplifying a green and cost-effective approach[25,26].

Comparative studies underscore the superior performance of these nanoparticles in terms of reusability. For instance, zinc oxide (ZnO) nanoparticles exhibit an 88% degradation efficiency upon reuse, while tin dioxide (SnO_2) nanoparticles demonstrate a degradation rate of 90%. Moreover, $Zr_2Ni_1Cu_7$ and $Zr_2Ni_1Cu_7/Si_3N_4$ nanoparticles achieve an impressive degradation efficiency of 92%[27-29]. Similarly, copper-cobalt-nickel (Cu-Co-Ni) nanoparticles exhibit a notable degradation capability of 92% reported by Abdulmohsen Ali Alshehri et al. These findings collectively highlight the efficacy and potential of the synthesized nanoparticles as versatile and sustainable photocatalysts for environmental remediation applications[30].

3.3.Antibacterial Activity:

The antibacterial efficacy of Te-loaded CuO, Ag, and Gd2O3 nanoparticles (NPs) was assessed against microbial strains including E. coli, S. pyogenes, S. aureus, and K. pneumonia at varying concentrations. The maximum inhibition concentration (MIC) against different pathogens is presented in Fig.3.3.2 and Fig.3.3.1. provides a graphical representation of the antibacterial activity of Te-loaded CuO, Ag, and Gd2O3 NPs against various bacterial pathogens, illustrating their potential as effective antimicrobial agents.

The bioactivity of these NPs is attributed to their ability to disrupt cellular mechanisms, induce DNA damage, and generate reactive oxygen species such as peroxides and superoxides, ultimately leading to denaturation of essential cellular components and enzyme inactivation. This multifaceted mechanism enables the suppression or eradication of bacterial growth by penetrating the cell membrane and inducing cellular death. Notably, hybrid nanoparticles exhibit enhanced antibacterial activity compared to individual nanoparticles reported by Hussain Sharma et al.

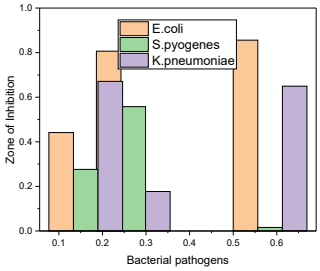

Fig. 3.3.1. shows the graphical representation of the antibacterial activity of Te-loaded CuO/ Ag/ Gd2O3 NPs against pathogens(E.coli, S.pyogenes,S. aureus,K.pneumonia) .

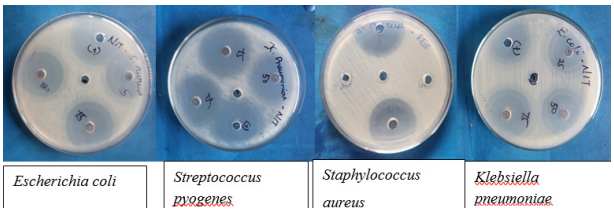

4. IN-VITRO ANTIMALARIAL ACTIVITY (Anti-Larvicidal Studies):

4.1. **Mosquito culture:**Aedes aegypti larvae were sourced from stagnant water areas in Thanjavur and identified using the available identification guide to the Medically Important Mosquito Species of EUCOM by David Pecor [32].

The larvae, along with the colony, were housed in plastic trays filled with tap water. The environmental conditions were carefully regulated, maintaining a temperature of 27 ± 2°C and relative humidity between 75–85%, with a light-dark cycle of 14:10 hours. The larvae were provided with a diet comprising Brewer's yeast, dog biscuits, and algae collected from ponds in a ratio of 3:1:1, respectively, following established protocols [33].

4.2.Larvicidal activity:

The larvicidal activity was evaluated following the procedure outlined by the World Health Organization (WHO) in 1996, with some modifications as described in the method [34].

For the bioassay, larvae were divided into five groups of 20 individuals each and placed in 100 ml of sterilized double-distilled water containing nanoparticles (NPs). A control group was maintained

with dechlorinated tap water. During the laboratory assessment, synthesized NPs underwent a dose-response bioassay to determine their larvicidal efficacy against Aedes aegypti.

Various concentrations of NPs, ranging from 5 to 25 mg/L, were prepared for the larvicidal assay. After 24 hours of exposure, the number of dead larvae was recorded, and the percentage mortality was calculated based on the average of three replicates. However, it was observed that, at the end of the 24-hour period, the selected test samples exhibited equal toxicity levels [35].

4.3.Statistical analysis:

Probits were analyzed using SPSS version 20, and the regression equation and r2 value were calculated logarithmically. The average larval mortality data underwent probit analysis to determine LC50, along with other statistics, at 95% fiducial limits of the upper confidence limit and lower confidence limit [36–40].

In this study, the larvicidal activity of synthesized Te-loaded CuO, Ag, and Gd_2O_3 nanoparticles (NPs) was evaluated. The results indicated varying levels of mortality, with synthesized PNs exhibiting 15%, 25%, 45%, 70%, and 85% mortality against Aedes aegypti at concentrations of 5, 10, 15, 20, and 25 mg/L, respectively (Figure 4.1 and Table 4.2). Notably, the highest mortality rate was observed in synthesized Te-loaded NPs against Aedes aegypti larvae at a concentration of 25 mg/L.

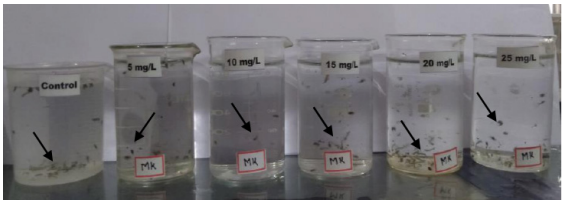

Fig. 4.1. Experimental step-up of larvicidal activity of Te-loaded CuO, Ag, and Gd2O3NPs using J. adhutoda against Aedes aegypti larvae (the arrow mark indicates the larvae).

The larvicidal activity of synthesized Te-loaded NPs yielded an LC50 (LCL-UCL) value of 13.583 (11.13–17.50) mg/L, with an r2 value of 0.9061 against Aedes aegypti (Figure 4.3 and Table 4.4). The observed lethal effects and mortality were dose-dependent, with the nanoparticles exhibiting heightened toxicity at higher concentrations (25 mg/L) against A. aegypti larvae.

Probits were analyzed using SPSS version 20, with the regression equation and r2 value calculated logarithmically. Concentration versus probit value was plotted, with a significance level set at alpha 0.05. The lower confidence limit (LCL) and upper confidence limit (UCL) were determined at 95% confidence.

The larvicidal activity of Ag nanoparticles (NPs) was particularly noteworthy across various developmental stages of Anopheles stephensi and Aedes aegypti. LC50, representing the lethal concentration at which 50% mortality occurs, was assessed, alongside the upper confidence limit (UCL) and the degree of freedom (df) [45].

Concentration (mg/L)	Log_{10} base concentration (mg/L)	Number of exposed larvae	24 Hours (MK)		
			Number of mortality	% of mortality	Probits
5	0.698	20	3	15	3.96
10	1.000	20	5	25	4.33
15	1.176	20	9	45	4.87
20	1.301	20	14	70	5.52
25	1.397	20	17	85	6.04

Table.4.3.Larvicidal activity of Te Loaded CuO/Ag/Gd_2O_3 NPs against Aedes aegyptilarvae .

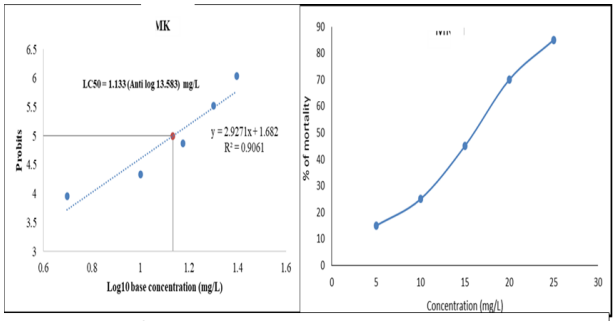

Fig:4.4. Calculation of LC_{50} value using Probit analysis and 4.5.Mortality curve of Aedes aegypti larvae following exposure to five concentrations (5, 10, 15, 20 and 25 mg/L in distilled water) ofsynthesized PNs.

Table : LC_{50} value

24 Hours	LC_{50} value (mg/L)			Regression equation	r^2 value
	LC_{50}	LCL	UCL		
Te Loaded Cu/Ag/Gd2O3	13.583	11.132	17.508	y = 2.9271x + 1.682	0.9061

Number of dead larvae/ pupa

Percentage(mortality) = No. of pupa or larvae introduced

The antiplasmodial effect was evaluated by administering increasing doses of Ag nanoparticles (NPs) ranging from 0.6 to 7.5 µg/ml on parasitized blood cells. It was observed that these nanoparticles promoted the maturation of Plasmodium falciparum. Notably, the in vitro antimalarial activity against P. falciparum was found to be effective at 0.90 µg/ml, underscoring the potent antimalarial activity of CuO NPs. Additionally, green-synthesized CuO NPs exhibited significant efficacy against dengue vectors Aedes aegypti and Anopheles stephensi, with observed LC50 values of 4.06 and 3.69 µg/ml, respectively [14].

Furthermore, heterocyclic organotelluranes demonstrated promising antimalarial activity against P. falciparum, with LC50 values recorded at 10 µm [33]. S

imilarly, Te-loaded CuO/Ag/Gd2O3 NPs exhibited notable efficiency against the malarial vector Aedes aegypti, thus suggesting their potential as antimalarial agents.

7.CONCLUSION :

It is evident that Te-loaded CuO, Ag, and Gd2O3 nanoparticles exhibit superior properties compared to their mono- and dimetallic counterparts. The distinct characteristics of these biofabricatedtetrametallic nanoparticles set them apart from conventional methods, allowing for customization of size and other attributes through the use of medicinal plants. Notably, these nanoparticles demonstrate remarkable antimalarial activity, surpassing that of individual compounds. Given their immense potential, they hold promise as safe and effective drug carriers for malaria treatment, particularly in addressing complications arising from drug-resistant strains. Importantly, these nanoparticles exhibit high selectivity in targeting infected cells while being safely eliminated from the host without compromising the immune system. Such attributes underscore their potential significance in combating malaria and related diseases.

References:

1. https://www.WHO.Org.in
2. National Center for Vector-Born Diseases Central, Ministry of Health and Family Welfare,GOI.
3. Zhibai Huang, Xiaoli Jiang, Dawei Guo, and Ning Gu,''Controllable Synthesis and Biomedical applications of Silver Nanomaterials;Journal of Nanoscience and Nanotechnology, VolII,9395-9408,2011.
4. Bell D, Wongsrichanalai E, and Barnwell JW, ''Ensuring quality and access for malaria diagnosis: how can it be achieved?'' Nat Rev Microbiol, 2006; 4:682-95.
5. Mercury CK, Gasser RA, Jr., Magil AJ, and Miller RS, ''Update on rapid diagnostic testing for malaria'', Microbiol Rev. 2008;21:97–110.
6. Christophe Hano, and Bilal Haider Abbasi, Plant-Based Green Synthesis of Nanoparticles: Production, Characterization and Applications. Biomolecules 2022,12,31.
7. .MC Gregor IA,Mechanism of Acquired Immunity and Epidemiological Patterns of Antibody Responses in Malaria in Man, Bull World Organ. 1974;50:259–66.
8. Devalapathy, A.Chaiklam,M.M.Amiji,''Role of nanotechnology in pharmaceutical product development, J.Pharm.sci.96(2007) 2547-2565.
9. Nereide Stola Santos-Magalhaes, Vanessa Carla, and Fernando Mosqueira, ''Nanotechnology applied to the treatment of malaria'', 2010, 560–575.
10. Mayra Aparecida Nasimento,Jean Castro Cruz, Mariana Ferreira dos Reis,Odilaine Inacio de Carvalho Damaceno,Efraim Lazaro Reis, Casa Reis, André Fernando de Oliveira, and Renata Pereira Lopes, ''Synthesis of Polymetallic Nanoparticles from Printed Circuit Board Waste and Application in Textile Dye Remediation, 2018
11. Jayaseelan,AhmedAbdulhaq,Chinnasamy Ragavendran, and Syam Mohan, ''Phytoconstituents-Assisted Biofabrication of Copper Oxide Nanoparticles and Their Antiplasmodial and Antilarval Efficacy:A Novel Approach for Control of Parasites'', 2022. Chidamabaram
12. 'Mahendra Rai,Avinash P. Ingle, PritiParalikar, IndarchandGupta, Serenella Medici, and Caroline A. Santas, ''Recent advances in the use of silver nanoparticles as antimalarial aganets, S0378-5173(17)30344-7.
13. Edward R. Tiekpink, ''Therapeutic potential of selenium and tellurium compounds: opportunities get unreacted'', 2012, 41, 6390.
14. Mahmoud Nazrollahzadeh,MohaddesehSajjadi,Siavash Iravani, and Rajender S.Varma, ''Trimetallic Nanoparticles: Greener Synthesis and Applications.
15. Ajeet nkitaGautam,BikarmaSingh,Navneet,Chapter 2: Antiviral effects of medicinal plants and their active phytochemical constituents against respiratory diseases and associated biological functions,2022, pages 23–54.
16. Nath, D.,Banerjee, P., ''Green nanotechnology: A new hope for medical biology'', Environ,Toxicol, and Pharmacol, 2013, 36, 99–1014.
17. Pritam Kumar Dikshit, Jatin Kumar,AmitkDas,Saumi Sadhu, SunitanSharma,SwathiSingh,Piyush Kumar Gupta, and Beom Soo Kim, ''Green Synthesis of Metallic Nanoparticles: Applications and Limitations.
18. Chandran .M., Pasricha.R, Ahmad.A,Sastry.M,''Synthesis of gold nanotriangles and silver nanoparticles using Aloevera plant extract'',Biotrechnol,Progr.,2006,22,577–583.
19. V,Herrera.I,Jose-Yacaman.M,Troiani.H,Santiago.P,Gardea-Terresday.J.L.,''Size-controlled gold nanoparticle formation by Avena sativa biomass: Use of plants in Nanobiotechnology, J.Nanoparticle.Res,2004,6,377-382.
20. Shimaa Hussein,Ayman M. Mahmoud,Hassan A. Elgebaly,Omnia Magdy Hendawy,Emad H.M. Hassanein,Shaima M.N. Mustafa,Nassar F. Alotaibi, and Amr M. Nassar,''GreenSyntheis of Trimetallic Nanocomposite (Ru, Ag, and Pd)-NP and its Invitro Antimicrobial and Anticancer Activities'',2022.
21. Yogesh B.Aher,GotanH.Jain,GaneshK.Ghotekar, DattaprasadM.Pore, ShreyasS. Pansambal,KeshawK. Deshmukh,''Biosynthesis of copper oxide nanoparticles using leaf extracts of Leucaena leucocephala L. and their promising upshort the selected human pathogens''.
22. Zahra Vaseghi,Omid Tavakoli, and Ali Nematollahzadeh, Rapid biosynthesis of novel Cu/Cr/Ni trimetallic oxide nanoparticles with antimicrobial activity,(2018), 1898–1911.
23. Bijan Zare,Mohammad Ali Faramarzi, ZaghamSepehrizadeh, and MojitabaShakibaie: Biosynthesis and recovery of rod-shaped tellurium nanoparticles and their bactericidal activities'', (2012), 3719–3725.
24. Q Liyuan,H Yong Yin, and Q Lin Nie,''Nnaostructured tellurium semiconductor: from nanoparticles to nanorods, 2013(7-8),937-936.
25. AgbajiLateef,Joseph A. Elegbede,Paul O. Akinola, and Victoria A. Ajayi, ''Biomedical Applications of Green Synthesized Metallic Nanoparticles: A Review''.
26. YingminJin, YunjanJiang, XinZong,Yumeng Li, and Yueping Xiong, Enhanced electrochemical performance and operating stability of LaO.8Sr.2CoO.2FeO.8O3-filled cathode via GdO.2CeO.8O_1.9-δ coating for intermediate temperature solid oxide fuel cells''.
27. SureshmM; Sivasamy A.,Fabrication of graphene nanosheets decorated by nitrogen-doped ZnO nanoparticles with enhanced visible photocatalytic activity for the degradation of methylene blue dye, 2020, 317, 114112. ina,S.K.,Lin,QingT,DongE,Li,Y;Irfan,M;Zhnag.P,''Fast photocatalytic degradation of dyes using low-power laser-fabricated Cu_2O-Cu nanocomposites'',RSC Adv.,2018,20277–20286.
28. Tammina,S.K.,Lin,Q.gT,DongE,Li,Y;Irfan,M;Zhnag.P,''Fast photocatalytic

degradation of dyes using low-power laser-fabricated Cu_2O-Cu nanocomposites'',RSC Adv.,2018,20277–20286.
29. SureshmM; Sivasamy A.,Fabrication of graphene nanosheets decorated by nitrogen-doped ZnO nanoparticles with enhanced visible photocatalytic activity for the degradation of methylene blue dye, 2020, 317, 114112.
30. G,Kumar.A,Sharma.A,Naushand,Ahmad.T,AL-Saeedi,''Facile fabrication of Zr2Ni1Cu7 trimetallic nanoalloy and its composite with Si3N4 for visible light-assisted photodegradation of methylene blue'',2018,272,170-179.
31. Abdulmohsen Ali Alshehri and Maqsood Ahmad Malik,''Facile one-pot synthesis of Cu-Co-Ni trimetallic nanoparticles for enhanced photocatalytic dye degradation, 2020.
32. David Pecor. (2020) Identification Guide to the Medically Important Mosquito Species of EUCOM Bionomics Diagnostic Morphological Characters Medical Importance Distribution
33. Kamaraj C, Bagavan A, Rahuman AA, Zahir AA, Elango G, and Pandiyan G. Larvicidal potential of medicinal plant extracts against Anopheles subpictusGrassi and CulextritaeniorhynchusGiles (Diptera: Culicidae) Parasitol Res. 2009;104:1163–71.
34. Velayutham, K., Rahuman, A. A., Rajakumar, G., Roopan, S. M., Elango, G., Kamaraj, C., & Siva, C. (2013). Larvicidal activity of green synthesized silver nanoparticles using a bark aqueous extract of Ficus racemosa against Culex quinquefasciatus and Culex gelidus. Asian Pacific Journal of Tropical Medicine, *6*(2), 95–101.
35. Benelli, G. (2016. Plant-mediated biosynthesis of nanoparticles as an emerging tool against mosquitoes of medical and veterinary importance: a review. Parasitol. Res. 115 (1), 23–34.
36. Parthiban, E., Ramachandran, M., Jayakumar, M., and Ramanibai, R., 2019. Biocompatible green synthesized silver nanoparticles impact insecticide-resistant developing enzymes of dengue-transmitted mosquito vectors. SN Appl. Sci. 1.
37. Shahzad, K., Manzoor, F., 2019. Nanoformulations and their mode of action in insects: a review of biological interactions. Drug & Chem. Toxicol. 44, 1–11.
38. Kalimuthu, K., Panneerselvam, C., Chou, C., Tseng, L.C., Murugan, K., Tsai, K.H., Alarfaj, A.A., Higuchi, A., Canale, A., Hwang, J.S., and Benelli, G., 2017. Control of dengue and Zika virus vector Aedes aegypti using the predatory copepod Megacyclopsformosanus: synergy with Hedychium coronarium-synthesized silver nanoparticles and related histo-logical changes in targeted mosquitoes. Process, Safety, and Environment, Prot. 109, 82–96.
39. 53.Madanagopal ySumathi,ChandranSundaravadivelan, ''Effect of Phyto-synthesized Silver Nanoparticles on the Development Stages of the Malaria Vector,Anophelesstephensi,and Dengue Vector,Aedes aegypti,(2017) 212-218.
40. Abekovan,Atamuarator, F.N., Erasheva, S.M., Turabeevsh.M,Sagdullaev B.T., ''Study of the spectrum characteristics of sulfamethoxazole-spectin by UV-Spectroscopy''.